HHS Public Access

Author manuscript

Anal Chim Acta. Author manuscript; available in PMC 2018 July 11.

Published in final edited form as:

Anal Chim Acta. 2017 July 11; 976: 63–73. doi:10.1016/j.aca.2017.04.014.

Chloroformate Derivatization for Tracing the Fate of Amino Acids in Cells and Tissues by Multiple Stable Isotope Resolved Metabolomics (mSIRM)

Ye Yang[a,b], **Teresa W-M. Fan**[a,b], **Andrew N. Lane**[a,b], and **Richard M. Higashi**[a,b]

[a]Center for Environmental and Systems Biochemistry, University of Kentucky, Lexington, KY, 40539

[b]Department of Toxicology and Cancer Biology, University of Kentucky, Lexington, KY, 40539

Abstract

Amino acids have crucial roles in central metabolism, both anabolic and catabolic. To elucidate these roles, steady-state concentrations of amino acids alone are insufficient, as each amino acid participates in multiple pathways and functions in a complex network, which can also be compartmentalized. Stable Isotope-Resolved Metabolomics (SIRM) is an approach that uses atom-resolved tracking of metabolites through biochemical transformations in cells, tissues, or whole organisms. Using different elemental stable isotopes to label multiple metabolite precursors makes it possible to resolve simultaneously the utilization of these precursors in a single experiment. Conversely, a single precursor labeled with two (or more) different elemental isotopes can trace the allocation of e.g. C and N atoms through the network.

Such dual-label experiments however challenge the resolution of conventional mass spectrometers, which must distinguish the neutron mass differences among different elemental isotopes. This requires ultrahigh resolution Fourier transform mass spectrometry (UHR-FTMS). When combined with direct infusion nano-electrospray ion source (nano-ESI), UHR-FTMS can provide rapid, global, and quantitative analysis of all possible mass isotopologues of metabolites. Unfortunately, very low mass polar metabolites such as amino acids can be difficult to analyze by current models of UHR-FTMS, plus the high salt content present in typical cell or tissue polar extracts may cause unacceptable ion suppression for sources such as nano-ESI.

Here we describe a modified method of ethyl chloroformate (ECF) derivatization of amino acids to enable rapid quantitative analysis of stable isotope labeled amino acids using nano-ESI UHR-FTMS. This method showed excellent linearity with quantifiable limits in the low nanomolar range represented in microgram quantities of biological specimens, which results in extracts with total analyte abundances in the low to sub-femtomole range. We have applied this method to

Correspondence to: Richard M. Higashi, rick.higashi@uky.edu Ph: 859-218-1027, Center for Environmental and System Biochemistry, University of Kentucky, Suite 521, Biopharm. Bldg.,789 S. Limestone St., Lexington, KY, 40539, USA; Teresa W.-M. Fan, teresa.fan@uky.edu, Ph: 859-218-1028, Center for Environmental and Systems Biochemistry, University of Kentucky, Suite 523, Biopharm. Bldg.,789 S. Limestone St., Lexington, KY, 40539, USA.

profile amino acids and their labeling patterns in ^{13}C and ^{2}H doubly labeled PC9 cell extracts, cancerous and non-cancerous tissue extracts from a lung cancer patient and their protein hydrolysates as well as plasma extracts from mice fed with a liquid diet containing $^{13}C_6$-glucose.

The multi-element isotopologue distributions provided key insights into amino acid metabolism and intracellular pools in human lung cancer tissues in high detail. The ^{13}C labeling of Asp and Glu revealed de novo synthesis of these amino acids from $^{13}C_6$-glucose via the Krebs cycle, specifically the elevated level of $^{13}C_3$-labeled Asp and Glu in cancerous versus non-cancerous lung tissues was consistent with enhanced pyruvate carboxylation. In addition, tracking the fate of double tracers, ($^{13}C_6$-Glc + $^{2}H_2$-Gly or $^{13}C_6$-Glc + $^{2}H_3$-Ser) in PC9 cells clearly resolved pools of Ser and Gly synthesized de novo from $^{13}C_6$-Glc ($^{13}C_3$-Ser and $^{13}C_2$-Gly) versus Ser and Gly derived from external sources ($^{2}H_3$-Ser, $^{2}H_2$-Gly). Moreover the complex ^{2}H labeling patterns of the latter were results of Ser and Gly exchange through active Ser-Gly one-carbon metabolic pathway in PC9 cells.

Graphical abstract

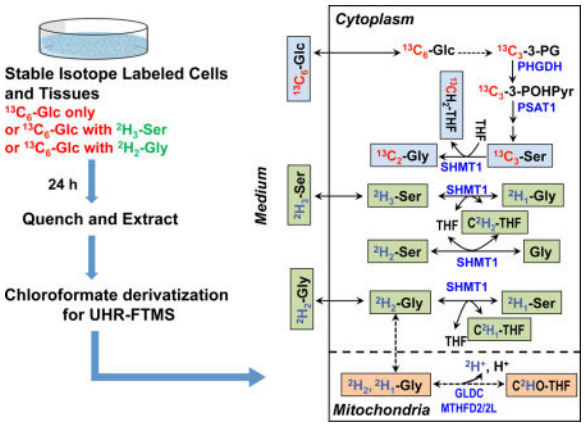

Keywords

Ultrahigh Resolution Fourier Transform Mass Spectrometry; Stable Isotope Resolved Metabolomics; Amino Acids; Direct infusion nano-electrospray

1. Introduction

1.1 Importance of amino acid metabolism

Amino acids play crucial roles in anabolic and catabolic metabolism. Not only are they the building blocks of proteins, they also are precursors to many key metabolites and oxidized to provide metabolic energy [1]. It was reported that amino acids account for the majority of dry cell mass in proliferating mammalian cells [2]. The non-essential amino acids Ala, Asp, and Glu play important roles in nitrogen metabolism via transamination, along with Arg, Orn, and citrulline in the urea cycle. Ser, Gly, Gln, and Asp are precursors in nucleotide synthesis, providing both carbon (Asp, Gly) and nitrogen (Gln, Asp) to the nucleobases [3]. Gln is also the nitrogen donor in the synthesis of amino sugars [4]. Arg, Orn, and Met are

also precursors of polyamines, which are essential in stress tolerance and nucleic acid function [5, 6]. These are just a few out of hundreds of vital metabolic roles of amino acids.

1.2 Stable Isotope-Resolved Metabolomics (SIRM) for robust pathway tracing

It is therefore crucially important to quantify amino acids to measure changes in concentrations and help determine their transformation pathways. The metabolic information contained in steady-state concentrations of metabolites, however, is often very limited, as each metabolite usually participates in multiple pathways, and most pathways are parallel, branched, reversible, and/or intersecting with each other to form a complex network. Thus, to robustly discern the precursor-product relationships for metabolic functions, it is necessary to "label" selected atoms in given metabolites so that their fates can be traced through metabolic pathways. Although radioisotopes such as ^{14}C were popular tracers in the past [7–9], many studies now use stable isotopes since they are nonhazardous for ease-of-use, and key elements can be readily observed by both NMR (e.g. ^{13}C and ^{15}N) and MS, given sufficient sensitivity and resolution of the instruments [10, 11]. We have coupled stable isotope tracers with NMR and MS analysis in stable isotope-resolved metabolomics (**SIRM**) to track the provenance of individual atoms through various transformation pathways in cells, tissues and whole organisms (including human subjects) while still achieving wide metabolome coverage [10, 12–16]. By determining the label position (isotopomer) and number (isotopologue) distribution in the various metabolites, SIRM generates the information that is used to reconstruct the turnover in pathways and abundances of newly synthesized metabolites with low ambiguities, providing a solid foundation for metabolic flux determination [17–19].

1.3. Need for ultrahigh resolution Fourier transform mass spectrometry (UHR-FTMS)

Using multiple precursors, each with distinct stable isotopes, makes it possible to simultaneously discern intersecting, cyclical, and even compartmentalized pathways in a single experiment, thereby providing novel insights into metabolic networks as perturbed by disease or other stressors. For example, administering $^{13}C_6$-glucose and $^{2}H_2$-Gly simultaneously to a biological system would enable not only tracing of glycolysis, the Krebs cycle, pentose phosphate pathway (PPP), nucleotide synthesis, and one carbon metabolism pathway but also delineation of the fate of de novo synthesized or exogenously derived Gly. Interpretations would be initially based on well-established networks [20].

Stable isotopes such as ^{13}C, ^{15}N, and ^{2}H differ from their most abundant isotopes by a single neutron. The apparent mass of a neutron in the nucleus differs slightly for each element due to differential nuclear binding energy [21]. The resulting mass difference for a molecule where ^{12}C was substituted by ^{13}C, versus ^{14}N substituted by ^{15}N, is too small to be resolved by the common "high resolution" mass spectrometers such as time-of-flight (TOF) MS with a maximum mass resolution (which is generally defined as m1/(m1-m2), where m1 and m2 are two peaks of equal intensity with less than 10% overlap, and by convention stated for an m/z such as 400 [22]) up to about 60,000. Instead, they can be distinguished using sufficiently high m/z resolution, as afforded by certain models of Fourier transform mass spectrometers (FTMS) [10, 13]. In practice, we have found that UHR-FTMS with a minimal resolving power in excess of 200,000 (at 400 m/z, 10% valley) is required [13, 22], and

usually a resolving power of 400,000 or more is needed [22–25]. In addition to “ultra” high resolution, all current models of UHR-FTMS instruments are capable of high m/z accuracy (<0.2 ppm RMS error with external calibration) for operative assignment of molecular formula candidates, yet have high sensitivity permitting quantification of analytes at low femtomole abundance in a sample [10].

1.4 Considerations of analyte derivatization for chromatography versus direct infusion UHR-FTMS

Most, if not all, MS-based analytical methods reported for quantitative analysis of amino acids in biological systems have been in combination with gas-liquid chromatography (GC) or liquid chromatography (LC). *N*-(*tert*-butyldimethylsilyl)-*N*-methyltrifluoroacetamide, introduced by Fan et al. in 1986 for GCMS analysis of organic and amino acids [26], has been a widely used silylation method for GC-based quantification of amino acids in biological materials. This method provides a high yield of molecular-ion isotopologue patterns under electron ionization [26–28], making it well suited for SIRM studies. Subsequently, Husek [29] reported a method of derivatizing amino acids with ethyl chloroformate (ECF) and demonstrated the fast analysis of amino acids by GCMS. Other researchers then modified the ECF derivatization method and applied it to a variety of materials including food, plant and urine samples [30, 31]. 9-Fluorenylmethyl-chloroformate (Fmoc-Cl) coupled with high performance liquid chromatography (HPLC) or fluorescence detection was also used to analyze amino acids in fruit juices and hydrolyzed peptides [32, 33]. Related reagents such as isobutyl chloroformate, methyl chloroformate, pentafluorobenzyl chloroformate have also been reported in amino acids analysis using GCMS or LCMS [34–36], although none of these were intended for use with SIRM.

With chromatography sample introduction to the MS, the short duration of each analyte available to the MS limits signal averaging, often causing critical isotopologues to be undetected [25]. In addition, the rapidly changing concentrations presented to the MS from chromatography compromises the quality of isotopologue data required for accurate and reproducible quantification. In contrast, through extensive signal averaging, the continuous infusion UHR-FTMS acquisition can provide high quality spectra rapidly with expanded dynamic range and accurate molecular formulae. Among the direct infusion methods, we have chosen the nano-electrospray ionization source (nano-ESI) because of its high sensitivity and capability of small sample consumption (typically 15 μL) and negligible sample waste. The latter is crucial to the increasing demand for microanalysis of cell or tissue samples (particularly those from human subjects), which is a result of sample size limitations such as the need to share the same biospecimens with other analyses such as genomics, transcriptomics, and proteomics, plus a wide range of biological assessments needed for interpretation, i.e. immunohistochemistry. For these reasons, UHR-FTMS coupled with nano-ESI has been a high priority for SIRM studies.

1.5 Limitations of direct infusion FTMS analysis of amino acids can be overcome by derivatization

Nano-ESI-UHR-FTMS has been successfully applied to analyze lipids, nucleotides, and other metabolites in SIRM studies [10, 13, 23]. Despite this versatility, it has been difficult

to detect some low m/z and/or polar metabolites such as amino acids and polyamines in crude cell extracts because of the ion suppression and instability of any ESI ion source caused by the high salt content inherent in crude cell or tissue extracts. This increases sample consumption, compromises sample throughput due to re-analyses, and interferes with quantitative data analysis. Furthermore, all current UHR-FTMS models are optimized for analytes with m/z greater than 150, compromising performance for smaller m/z metabolites. These problems are exacerbated by the need to analyze numerous isotopologues present at very low abundance in SIRM experiments, even abundant metabolites whose monoisotopic species are readily detected by UHR-FTMS can have low enrichment isotopologues crucial for biochemical interpretation. Lastly, the biochemical liability of some metabolites makes them impractical to quantify with confidence. Therefore, there is a need to develop a suitable derivatization method for these small metabolites for nano-ESI-UHR-FTMS analysis.

In this report, we have coupled ECF derivatization with nano-ESI-UHR-FTMS for microanalysis of amino acids. ECF can derivatize both $–NH_2$ and –COOH groups on amino acids. After the ECF derivatization, all amino acids have an m/z greater than 170, which makes them suitable for UHR-FTMS analysis by current models. The derivatives are also more hydrophobic and can be extracted by chloroform to eliminate the salt effect. The derivatization can also stabilize some labile amino acids such as Gln. We applied the method to analyze the stable isotopologue distribution in polar extract of various isotope-labeled biological samples including single-opportunity surgical lung cancer patient tissues, lung cancer cells, patient-derived mouse xenograft tissues, hydrolyzed protein samples from these sources, and human plasmas.

2. Materials and Methods

2.1 Reagents

All unlabeled amino acid standards were purchased from Sigma Aldrich (St. Louis, MO) as a mixture of acidic and neutral amino acids (A6407) and basic amino acids (A6282). Gln, ethyl chloroformate (ECF), ethanol, pyridine and chloroform were also purchased from Sigma Aldrich. The uniformly ^{15}N-labeled amino acids mixture was purchased from Cambridge Isotope Laboratories (NLM-6695, Cambridge, MA).

2.2 Methods

2.2.1 Preparation of amino acid standards—Immediately prior to analysis, the amino acids mixtures A6407 and A6282 were combined in equal volumes before experiments, and then a freshly prepared aqueous solution of Gln solution was added. In the final solution, the concentration of each amino acid was 0.556 mM except cystine, which was 0.278 mM. This stock was then serially diluted to concentrations of 0.278 mM, 0.111 mM, 0.056 mM, 0.028 mM, 0.011 mM, 0.0056 mM and 0.0011 mM.

2.2.2 Preparation of unlabeled PC-9 cell polar extract—Human lung adenocarcinoma PC-9 cells were grown on 10 cm cell culture plates in Dulbecco's Modified Eagle's Medium (DMEM) containing 10% fetal bovine serum (FBS) (Life Technologies,

Carlsbad, CA), 50 U mL^{-1} penicillin (Thermo Fisher Scientific), 50 μg mL^{-1} streptomycin (Fisher Scientific, Waltham, MA), 0.2% unlabeled glucose (MP Biomedicals, LLC) for two days. Then the media was changed to DMEM media containing 10% dialyzed FBS (Life Technologies, Carlsbad, CA), 50 U mL^{-1} penicillin, 50 μg mL^{-1} streptomycin, 2 mM Gln (Sigma Aldrich), 0.45% glucose, 0.4 mM unlabeled Ser (Sigma Aldrich) and 0.4 mM unlabeled Gly (Sigma Aldrich). After 24 h, the cells were quenched, harvested and extracted with CH_3CN:H_2O:$CHCl_3$ (2:1.5:1) [37]. Then the aqueous phase containing polar extracts was distributed into aliquots and lyophilized for ECF derivatization.

2.2.3 Preparation of plasma polar extract from NOD/SCID/Gamma (NSG) mice fed with $^{13}C_6$- Glc enriched liquid diet—The NOD/SCID/Gamma (NSG) mice were fed with a custom liquid diet in which $^{13}C_6$-glucose is the primary carbohydrate source for 18 h as described previously [38]. The mice were then sacrificed and 20 μl of plasma was extracted twice with 600 μL acetonitrile:methyl *tert*-butyl ether (MTBE):H_2O (2:3:1) mixture to eliminate lipids [39]. Then the polar phase was deproteinized with 800 μL acetonitrile:acetone:methanol (8:1:1), followed by taking a 1/10 aliquot to lyophilize for ECF derivatization.

2.2.4 Preparation of lung cancer patient tissue polar extract—Both cancer tissues and surrounding non-cancer tissues of patients were collected in the operating room within 5 minutes of resection from patient UK018 under our University of Kentucky Internal Review Board (IRB) protocol (IRB 14-0288-F6A). The tissues were cut into thin slices at approximately 0.7 to 1 mm thickness each. Paired cancer and non-cancer tissue slices were collected and incubated in glucose, Gly and Ser-free DMEM medium (Life Technologies, Carlsbad, CA) with 10% dialyzed fetal bovine serum, 50 U mL^{-1} penicillin, 50 μg mL^{-1} streptomycin, 2 mM Gln, 0.4 mM Ser, 0.4 mM Gly and 0.45% $^{13}C_6$-Glc (Sigma, St. Louis, MO). The slices were cultured at 37 °C with 5% CO_2 for 24 h with gentle rocking as described [40]. The slices were quickly rinsed in cold PBS 3 times to remove any remaining media, vacuum aspirated, and then flash frozen in liquid N_2. The frozen tissue slices were then homogenized in 60% cold CH_3CN in a ball mill (Precellys-24, Bertin Technologies, Washington, DC, MD), then extracted with CH_3CN:H_2O:$CHCl_3$ (2:1.5:1) [37]. Again the aqueous phase containing polar extracts was distributed into aliquots and lyophilized for ECF derivatization.

2.2.5 Hydrolysis of proteins from human lung tissues—After polar and lipid extraction of the ground tissue sample, the protein pellet was dried in a vacuum centrifuge and then extracted with 62.5 mM tris(hydroxymethyl)aminomethane (Tris) (Fisher Scientific) with 2% sodium dodecyl sulfate (SDS) (Fisher Scientific), 1 mM dithiothreitol (DTT) (Fisher Scientific), pH 6.8 [37]. The protein solution was precipitated with 10% trichloroacetic acid (TCA) (Fisher Scientific) and washed twice with H_2O. Then the protein pellet was hydrolyzed in 6 N HCl with a focused beam microwave (CEM, Discover-SP, Matthews, NC, USA) at 160 °C for 10 min at a maximum power of 150 W, guided by previous work [41] and optimized by Y. Yang [42]. The hydrolyzed samples were then distributed into aliquots and lyophilized for ECF derivatization.

2.2.6 Preparation of double tracer labeled PC-9 cell polar extract—Human lung adenocarcinoma PC-9 cells were grown on 10 cm cell culture plates in DMEM containing 10% FBS, 50 U mL^{-1} penicillin, 50 μg mL-1 streptomycin, 0.2% unlabeled glucose for two days first. Then the media was changed to DMEM media containing 10% dialyzed fetal bovine serum, 50 U mL^{-1} penicillin, 50 μg mL^{-1} streptomycin and 2 mM Gln, and also with 0.45% $^{13}C_6$-Glc/0.4 mM unlabeled Ser/0.4 mM unlabeled Gly, or 0.45% $^{13}C_6$-Glc/0.4 mM $^{2}H_3$-Ser (Cambridge Iosotope Laboratories, Tewksbury, MA)/0.4 mM unlabeled Gly, or 0.45% $^{13}C_6$-Glc/0.4 mM unlabeled Ser/0.4 mM $^{2}H_2$-Gly (Cambridge Iosotope Laboratories, Tewksbury, MA) respectively for different isotope tracer groups. After 24 h, the cells were quenched, harvested and extracted with CH_3CN:H_2O:$CHCl_3$ (2:1.5:1) [37]. Then the aqueous phase containing polar extracts was distributed into aliquots and lyophilized for ECF derivatization.

2.2.7 ECF derivatization—For the amino acid standards, 9 μL of each amino acid standard sample was used at the concentration stated in section 2.2.1. For the cell/tissue/plasma polar extract, the freeze-dried fraction was used directly. H_2O/Ethanol/Pyridine (6:3:1) mixture (100 μL) was added, followed by 5 μL of ECF. The mixture was allowed to react by vortexing for 30 s. Chloroform (100 μL) was then added to extract the products followed by 10 μL of 7 M NaOH to adjust the aqueous layer to pH 9–10, after which a further 5 μL of ECF was added and allowed to react again for 30 s. The solution was extracted a second time with 100 μL chloroform, and combined with the first extract. The combined chloroform extract was diluted 100 fold for the amino acid standards and 10 fold for cell or tissue samples with acetonitrile/water (9:1) solution to a final concentration of 20 μM NaCl to convert the ions to their sodium adducts. The samples were then directly injected into the FTMS using nano-ESI for UHR-FTMS analysis.

2.2.8 Mass spectrometry and peak assignments—UHR-FTMS analysis was carried out using the Tribrid Fusion Orbitrap (Thermo Scientific, San Jose, CA, USA), interfaced with an Advion Triversa Nanomate (Advion Biosciences, Ithaca, NY, USA). The Nanomate was operated at 1.5 kV and 0.5 psi head pressure in positive ion mode. The maximum ion time for the automatic gain control (AGC) was set to 100 ms, acquiring 5 micro scans, and each sample was acquired for >5 min with m/z range 100–1000 selected using quadrupole isolation. For data analysis, a single spectrum was obtained for each sample by averaging spectra over the entire acquisition time.

All ^{12}C, ^{13}C, ^{15}N and ^{2}H isotopologue peaks were assigned using “PREMISE” (PRecalculated Exact Mass Isotopologue Search Engine) [13] based on their accurate m/z values and the natural abundance distribution of each isotopologue was corrected (or “stripped”) using the method developed by Moseley [43].

3. Results and discussion

3.1 Analysis of amino acid standards

The ECF derivatization method was first evaluated using the amino acid mixture (Figure A.1 and Table 1). NMR analysis established that the ECF reaction efficiency was between 82–99.9% for the amino acid standards (Table A.1), based on ^{15}N labeled amino acids added as

internal standards for quantification. Since these ^{15}N standards were added before reaction with ECF, the ratio between each amino acid and its spiked ^{15}N counterpart was used to correct for the reaction and extraction efficiency, thus enabling quantification of each amino acid and its ^{13}C labeled isotopologues despite lacking the actual reaction efficiency. Note that the use of UHR-FTMS enables the deployment of such isotopic surrogates as internal standards for biologically stable isotope labeled analytes. The ECF-derivatized amino acids were observed as sodium adducts except Arg, which was measured as the protonated form that dominated over the sodium adduct. For His and Lys, both protonated and Na adducts were present, but the Na adducts dominated at low concentrations.

For all amino acids tested, the UHR-FTMS quantification showed excellent linear response over more than three orders of magnitude with high sensitivity (Figure A.1 and Table 1), indicating that reliable absolute quantification of amino acids was achieved by this method. Leu and Ile are shown as a single entry as they are isobaric, and therefore are not resolved by direct infusion MS.

3.2 Analysis of amino acids in unlabeled polar extracts of PC9 cells

Direct analysis of cell extracts without derivatization by direct infusion nano-ESI UHR-FTMS was unsuccessful, even after 100-fold dilution to reduce the ion suppression. However, after ECF derivatization and chloroform extraction, the nano-ESI spray was stable for more than fifteen minutes, which readily enabled sensitive detection and reliable quantification of amino acids and their isotopologues. Figure 1 shows a typical positive-ion mode spectrum of a polar extract of PC9 cells after ECF derivatization and chloroform extraction. Small amino acids such as Gly and Ala were now detected with good sensitivity (at low femtomole levels), even though their underivatized forms were difficult to analyze by direct infusion-FTMS due to their low m/z values.

3.3 Analysis of amino acids in plasma from NOD/SCID/Gamma (NSG) mice fed with $^{13}C_6$-Glc enriched liquid diet

Figure 2 summarizes the ^{13}C enrichment of amino acids in mouse plasma after 18 h of feeding with $^{13}C_6$-glucose diet. We found that about a third of the Ala was $^{13}C_3$ labeled, and about half of Glu was ^{13}C labeled (sum of all ^{13}C isotopologues), indicating that about one third of Ala and one half of Glu in plasma was synthesized de novo from dietary glucose. The rationale is as follows: $^{13}C_3$-Ala is synthesized from $^{13}C_6$-Glc via the production of $^{13}C_3$-pyruvate through glycolysis followed by transamination. $^{13}C_3$-pyruvate can also enter the Krebs Cycle to produce $^{13}C_2$-α-ketoglutarate, which can in turn generate $13C_2$-Glu via the action either of glutamate dehydrogenase or glutamate-α-ketoglutarate aminotransferase. The $^{13}C_2$-Glu may subsequently be converted to $^{13}C_2$-Gln by glutamine synthetase. Additional cycling through the Krebs cycle can produce $^{13}C_3$-, $^{13}C_4$ -, $^{13}C_1$ - and $^{13}C_5$-α-ketoglutarate and thus generate $^{13}C_3$-, $^{13}C_4$ $^{13}C_1$ - and $^{13}C_5$-Gln via correspondingly labeled Glu. Glu, however, was present at low concentrations and showed very little ^{13}C enrichment (Figure 2), which suggests the majority of Glu originated from the diet rather than by de novo synthesis from glucose, and further, the majority of newly synthesized Glu was consumed for Gln synthesis. The total concentrations of amino acids

measured (the sum of all isotopologues) in mice plasma was comparable to values reported in the literature [44].

3.4. Analysis of free amino acids in $^{13}C_6$-Glc labeled tissue slices from a lung cancer patient

We obtained freshly resected cancerous (CA) and paired non-cancerous (NC) lung tissues from human subjects, which were thinly sliced and incubated in $^{13}C_6$-Glc containing DMEM media, as previously described [25, 40]. Figure 3 shows the isotopologues of selected amino acids determined in these tissue slices. The left three figures show the absolute quantification of amino acids in NC versus CA tissue extracts normalized to protein weight (nmole/mg protein) while the right three figures show the corresponding fractional enrichment. We found that after 24 h of incubation with $^{13}C_6$-Glc, about 14% Ala was synthesized de novo in NC tissues and 62% in CA tissues, which suggested higher glycolytic and aminotransferase capacity in CA tissues. This is consistent with the metabolic reprogramming shown previously [12]. In addition, $^{13}C_2$-Asp and $^{13}C_3$-Asp were synthesized, evidently via the pyruvate dehydrogenase (PDH) and pyruvate decarboxylase (PCB) reactions, respectively (Figure 4). The fractional enrichment data suggested that compared with paired NC tissue slices, CA tissue slices had a relatively higher capacity for PCB- than PDH-initiated Krebs cycle reactions, which was consistent with previous report [11]. Moreover, since $^{13}C_3$- and $^{13}C_4$-Glu can be produced from additional Krebs Cycle turns and $^{13}C_4$-Glu can be synthesized from the PCB activity (Figure 4), the relatively higher enrichment of these isotopologues in the CA versus NC tissue slices pointed to more active Krebs cycle in the CA tissues. This is consistent with a higher energy and carbon demand of cancer cells to support their survival and growth.

3.5 Analysis of proteinaceous amino acids from lung cancer patient UK018

We also extracted protein fractions from the tissue slices of the same patient described above. To determine the incorporation of ^{13}C labeled amino acids into proteins, we first hydrolyzed the protein extracts by microwave digestion using a modified method [41, 42] Independent of the hydrolysis efficiency, the fractional enrichment data of the isotopologues of each amino acid is reliable. Figure 5 shows the ^{13}C fractional enrichment in amino acids hydrolyzed from the protein fraction of the lung cancer patient (UK018) tissue slice experiment. While the essential amino acids were unlabeled in the protein pool as expected, we observed appreciable ^{13}C enrichment in non-essential amino acids, Glu, Ala, and Asp. The Glu and Asp data showed that the ^{13}C enrichment was significantly increased in proteins from the CA tissue slices compared to the NC counterparts. It should be noted that Glu represented Glu+Gln as acid hydrolysis converts Gln to Glu. This result indicates that amino acids synthesized de novo from glucose were incorporated into proteins, and that the capacity of protein synthesis was higher in CA than in NC tissues. True protein turnover would require measurements of synthesis and degradation rates, which can be obtained with the present method but is beyond the scope of this report.

3.6. Analysis of amino acids in polar extracts of PC9 cells grown on dual labeled sources

Stable isotope labeling is indispensible for robust mapping of metabolic pathways. Due to the complexity of metabolic networks, even the single tracer approach is often insufficient in

terms of biochemical resolving power and coverage for gaining a comprehensive understanding of the system. The use of UHR-FTMS enables freedom to design experiments that multiplex different isotopes in the same experiment, including ^{13}C, ^{15}N and ^{2}H (cf. Figure A2). We have grown PC9 cells in DMEM media for 24 h with $^{13}C_6$-Glc + $^{2}H_2$-Gly, or with $^{13}C_6$-Glc + $^{2}H_3$-Ser (see Methods) to distinguish the de novo synthesis of Ser and Gly (derived from $^{13}C_6$-Glc) from metabolism of exogenous ^{2}H labeled Ser or Gly present in the growth medium. Ser can be synthesized from glucose via the glycolytic intermediate 3-phosphoglycerate (3-PGA) and Ser can be subsequently converted to Gly by the action of serine hydroxymethyl transferase (SHMT), as shown in Figure 6. This Ser-Gly-one carbon pathway provides precursors for the synthesis of purines [3]. Thus the enrichment of Ser and Gly with ^{13}C is expected to proceed via this pathway. Both Ser and Gly, however, can be taken up from the medium, which can be simultaneously tracked using ^{2}H-labeled Ser or Gly in the medium. The SHMT-catalyzed exchange between Ser and Gly may lead to scrambling of the deuterium label, which is discerned by ECF derivatization UHR-FTMS analysis independently of the ^{13}C enrichment in the amino acids pools. Recent report has shown that Ser is more likely than Gly to support one-carbon metabolism and proliferation of cancer cells [45]. It is therefore crucial to understand the pools and fates of Ser and Gly in regard of cancer metabolism.

Figure 7 shows the Gly and Ser regions in the UHR-FTMS spectrum of a polar extract of dually labeled PC9 cells. The expanded region illustrates clear resolution of $^{13}C_2$ - from $^{2}H_2$-isotopologues of Gly, and $^{13}C_3$- from $^{2}H_3$-isotopologues of Ser, and Figure 8 shows the fractional enrichment results of these assigned isotopologue species. After 24 h of growth in labeled cell media, about 20 to 30% of Gly and Ser were labeled with ^{13}C only, which indicates de novo synthesis of Gly and Ser from glucose via glycolysis and the 3-PG pathway (Figure 6). A further 20–30% were ^{2}H labeled only, indicating that these amino acids were newly imported from the external medium. However, more than half of the exogenously derived $^{2}H_3$-Ser was converted to $^{2}H_2$- and $^{2}H_1$-Ser, while the main deuterated isotopologue of Gly was $^{2}H_1$-Gly when either $^{2}H_3$-Ser or $^{2}H_2$-Gly was present in the medium. As before, these scrambled products of Ser and Gly indicated extensive deuterium exchange processes between Ser and Gly via 1-carbon metabolism, as catalyzed by SHMT, glycine decarboxylase complex (GLDC), and methylenetetrahydrofolate dehydrogenase (MTHFD).

4. Conclusions

We have harnessed and modified the rapid ECF derivatization coupled with nano-ESI-UHR-FTMS method for microanalysis of amino acids. The resulting hydrophobic derivatives allowed use of chloroform extraction to minimize salt in polar extracts of biological samples, which avoided major matrix interferences. Together with the use of internal ^{15}N labeled amino acid standards, we achieved highly sensitive, rapid, and reliable quantification of amino acids without the need for chromatography. Isobaric compounds such as Leu and Ile are not resolved with this new method, which would require chromatographic separation. We have applied this method to analyze amino acids in a wide range of biological matrices including cells, tissues, biofluids, and their protein hydrolysates. This, in turn, demonstrated the ability of mass spectrometry at sub-atomic (neutron) resolution to resolve dual tracers

(^{13}C and ^{2}H) simultaneously present in amino acids, thereby opening new avenues for studies of metabolic networks at the atom-resolved level.

Supplementary Material

Refer to Web version on PubMed Central for supplementary material.

Acknowledgments

This work was supported in part by National Institute of Health [5R01ES022191-04, 3R01ES022191-04S1, 1U24DK097215-01A1 and P01 CA163223-01A1]. We thank Dr. Ronald Bruntz for the PC9 cell extraction, Ms. Yan Zhang for the UK022 tissue slice extraction, Dr. Ramon Sun for mouse sample preparation, and Dr. Penghui Lin for recording NMR spectra on the samples and for data reduction. We also thank Dr. Hunter Moseley for discussion of the natural abundance stripping.

Abbreviations

DMEM	Dulbecco's modified Eagle's medium
ECF	ethyl chloroformate
EI	electron ionization
PPP	pentose phosphate pathway
GC	gas chromatography
LC	liquid chromatography
nano-ESI	nano-electrospray ion source
SIRM	stable isotope resolved metabolomics
UHR-FTMS	ultrahigh resolution Fourier transform mass spectrometry
NMR	nuclear magnetic resonance
MS	mass spectrometry
HPLC	high performance liquid chromatography
GCMS	gas chromatography mass spectrometry
LCMS	liquid chromatography mass spectrometry

References

1. Lehninger, AL., Nelson, DL., Cox, MM. Lehninger principles of biochemistry. New York: Worth Publishers; 2000.
2. Hosios AM, Hecht VC, Danai LV, Johnson MO, Rathmell JC, Steinhauser ML, Manalis SR, Vander Heiden MG. Amino Acids Rather than Glucose Account for the Majority of Cell Mass in Proliferating Mammalian Cells. Dev Cell. 2016; 36(5):540–9. [PubMed: 26954548]
3. Lane AN, Fan TWM. Regulation of mammalian nucleotide metabolism and biosynthesis. Nucleic Acids Res. 2015; 43:2466–2485. [PubMed: 25628363]

4. Vogler AP, Trentmann S, Lengeler JW. Alternative route for biosynthesis of amino sugars in Escherichia coli K-12 mutants by means of a catabolic isomerase. J Bacteriol. 1989; 171(12):6586–92. [PubMed: 2687246]
5. Ha HC, Sirisoma NS, Kuppusamy P, Zweier JL, Woster PM, Casero RA Jr. The natural polyamine spermine functions directly as a free radical scavenger. Proc Natl Acad Sci U S A. 1998; 95(19): 11140–5. [PubMed: 9736703]
6. Sagor GH, Berberich T, Takahashi Y, Niitsu M, Kusano T. The polyamine spermine protects Arabidopsis from heat stress-induced damage by increasing expression of heat shock-related genes. Transgenic Res. 2013; 22(3):595–605. [PubMed: 23080295]
7. Lappin G. A historical perspective on radioisotopic tracers in metabolism and biochemistry. Bioanalysis. 2015; 7(5):531–40. [PubMed: 25826135]
8. Nelson DR, Zeikus JG. Rapid method for the radioisotopic analysis of gaseous end products of anaerobic metabolism. Appl Microbiol. 1974; 28(2):258–61. [PubMed: 4854029]
9. Sinzinger H, Rogatti W. Prostaglandins and arterial wall lipid metabolism–in vitro, ex-vivo and in-vivo radioisotopic studies. J Physiol Pharmacol. 1994; 45(1):27–40. [PubMed: 8043908]
10. Fan TW, Lorkiewicz PK, Sellers K, Moseley HN, Higashi RM, Lane AN. Stable isotope-resolved metabolomics and applications for drug development. Pharmacol Ther. 2012; 133(3):366–91. [PubMed: 22212615]
11. Sellers K, Fox MP, Bousamra M 2nd, Slone SP, Higashi RM, Miller DM, Wang Y, Yan J, Yuneva MO, Deshpande R, Lane AN, Fan TW. Pyruvate carboxylase is critical for non-small-cell lung cancer proliferation. J Clin Invest. 2015; 125(2):687–98. [PubMed: 25607840]
12. Fan TW, Lane AN, Higashi RM, Farag MA, Gao H, Bousamra M, Miller DM. Altered regulation of metabolic pathways in human lung cancer discerned by (13)C stable isotope-resolved metabolomics (SIRM). Mol Cancer. 2009; 8:41. [PubMed: 19558692]
13. Lane AN, Fan TW, Xie Z, Moseley HN, Higashi RM. Isotopomer analysis of lipid biosynthesis by high resolution mass spectrometry and NMR. Anal Chim Acta. 2009; 651(2):201–8. [PubMed: 19782812]
14. Ballevre O, Prugnaud J, Houlier ML, Arnal M. Assessment of threonine metabolism in vivo by gas chromatography/mass spectrometry and stable isotope infusion. Anal Biochem. 1991; 193(2):212–9. [PubMed: 1908193]
15. Bluck LJ. Recent progress in stable isotope methods for assessing vitamin metabolism. Curr Opin Clin Nutr Metab Care. 2009; 12(5):495–500. [PubMed: 19571745]
16. Vaitheesvaran B, Chueh FY, Xu J, Trujillo C, Saad MF, Lee WN, McGuinness OP, Kurland IJ. Advantages of dynamic “closed loop” stable isotope flux phenotyping over static “open loop” clamps in detecting silent genetic and dietary phenotypes. Metabolomics. 2010; 6(2):180–190. [PubMed: 20445758]
17. Lane AN, Fan TW, Bousamra M 2nd, Higashi RM, Yan J, Miller DM. Stable isotope-resolved metabolomics (SIRM) in cancer research with clinical application to nonsmall cell lung cancer. OMICS. 2011; 15(3):173–82. [PubMed: 21329461]
18. Foguet C, Marin S, Selivanov VA, Fanchon E, Lee WN, Guinovart JJ, de Atauri P, Cascante M. HepatoDyn: A Dynamic Model of Hepatocyte Metabolism That Integrates 13C Isotopomer Data. PLoS Comput Biol. 2016; 12(4):e1004899. [PubMed: 27124774]
19. de Mas IM, Selivanov VA, Marin S, Roca J, Oresic M, Agius L, Cascante M. Compartmentation of glycogen metabolism revealed from 13C isotopologue distributions. BMC Syst Biol. 2011; 5:175. [PubMed: 22034837]
20. Moseley HN, Lane AN, Belshoff AC, Higashi RM, Fan TW. A novel deconvolution method for modeling UDP-N-acetyl-D-glucosamine biosynthetic pathways based on (13)C mass isotopologue profiles under non-steady-state conditions. BMC Biol. 2011; 9:37. [PubMed: 21627825]
21. Greene GL, Kessler EG Jr, Deslattes RD, Borner H. New determination of the deuteron binding energy and the neutron mass. Phys Rev Lett. 1986; 56(8):819–822. [PubMed: 10033294]
22. Higashi, RM. The handbook of Metabolomics Methods in Pharmacology and Toxicology. Humana Press; 2012. Chapter 4: Structural Mass Spectrometry for Metabolomics.

23. Lorkiewicz PK, Higashi RM, Lane AN, Fan TW. High information throughput analysis of nucleotides and their isotopically enriched isotopologues by direct-infusion FTICR-MS. Metabolomics. 2012; 8(5):930–939. [PubMed: 23101002]
24. Higashi RM, Fan TW, Lorkiewicz PK, Moseley HN, Lane AN. Stable isotope-labeled tracers for metabolic pathway elucidation by GC-MS and FT-MS. Methods Mol Biol. 2014; 1198:147–67. [PubMed: 25270929]
25. Fan TW, Warmoes MO, Sun Q, Song H, Turchan-Cholewo J, Martin JT, Mahan A, Higashi RM, Lane AN. Distinctly perturbed metabolic networks underlie differential tumor tissue damages induced by immune modulator beta-glucan in a two-case ex vivo non-small-cell lung cancer study. Cold Spring Harb Mol Case Stud. 2016; 2(4):a000893. [PubMed: 27551682]
26. Fan TW, Higashi RM, Lane AN, Jardetzky O. Combined use of 1H-NMR and GC-MS for metabolite monitoring and in vivo 1H-NMR assignments. Biochim Biophys Acta. 1986; 882(2): 154–67. [PubMed: 3011112]
27. Schummer C, Delhomme O, Appenzeller BM, Wennig R, Millet M. Comparison of MTBSTFA and BSTFA in derivatization reactions of polar compounds prior to GC/MS analysis. Talanta. 2009; 77(4):1473–82. [PubMed: 19084667]
28. MacKenzie SL, Tenaschuk D, Fortier G. Analysis of amino acids by gas-liquid chromatography as tert.-butyldimethylsilyl derivatives. Preparation of derivatives in a single reaction. J Chromatogr. 1987; 387:241–53. [PubMed: 3558623]
29. Husek P. Amino acid derivatization and analysis in five minutes. FEBS Lett. 1991; 280(2):354–6. [PubMed: 2013337]
30. Mudiam MK, Ratnasekhar C, Jain R, Saxena PN, Chauhan A, Murthy RC. Rapid and simultaneous determination of twenty amino acids in complex biological and food samples by solid-phase microextraction and gas chromatography-mass spectrometry with the aid of experimental design after ethyl chloroformate derivatization. J Chromatogr B Analyt Technol Biomed Life Sci. 2012; 907:56–64.
31. Qiu Y, Su M, Liu Y, Chen M, Gu J, Zhang J, Jia W. Application of ethyl chloroformate derivatization for gas chromatography-mass spectrometry based metabonomic profiling. Anal Chim Acta. 2007; 583(2):277–83. [PubMed: 17386556]
32. Fabiani A, Versari A, Parpinello GP, Castellari M, Galassi S. High-performance liquid chromatographic analysis of free amino acids in fruit juices using derivatization with 9-fluorenylmethyl-chloroformate. J Chromatogr Sci. 2002; 40(1):14–8. [PubMed: 11866381]
33. Shangguan D, Zhao Y, Han H, Zhao R, Liu G. Derivatization and fluorescence detection of amino acids and peptides with 9-fluorenylmethyl chloroformate on the surface of a solid adsorbent. Anal Chem. 2001; 73(9):2054–7. [PubMed: 11354490]
34. Villas-Boas SG, Delicado DG, Akesson M, Nielsen J. Simultaneous analysis of amino and nonamino organic acids as methyl chloroformate derivatives using gas chromatography-mass spectrometry. Anal Biochem. 2003; 322(1):134–8. [PubMed: 14705791]
35. Deng C, Li N, Zhang X. Rapid determination of amino acids in neonatal blood samples based on derivatization with isobutyl chloroformate followed by solid-phase microextraction and gas chromatography/mass spectrometry. Rapid Commun Mass Spectrom. 2004; 18(21):2558–64. [PubMed: 15468143]
36. Simpson JT, Torok DS, Markey SP. Pentafluorobenzyl chloroformate derivatization for enhancement of detection of amino acids or alcohols by electron capture negative ion chemical ionization mass spectrometry. J Am Soc Mass Spectrom. 1995; 6(6):525–8. [PubMed: 24214307]
37. Fan, TW-M. Chapter 2: Considerations of Sample Preparation for Metabolomics Investigation. In: Fan, TW-M.Lane, AN., Higashi, RM., editors. The Handbook of Metabolomics. Springer Protocols; 2012.
38. Sun RC, Warmoes MO, Yang Y, Deng P, Sun Q, Lane AN, Higashi RM, Fan TWM. Noninvasive liquid diet delivery of stable isotopes into PDX mice for deep metabolic pathway tracing. Nature Communication. 2017 under review.
39. Matyash V, Liebisch G, Kurzchalia TV, Shevchenko A, Schwudke D. Lipid extraction by methyl-tert-butyl ether for high-throughput lipidomics. J Lipid Res. 2008; 49(5):1137–46. [PubMed: 18281723]

40. Fan TWM, Lane AN, Higashi RM. Stable Isotope Resolved Metabolomics Studies in ex vivo Tissue Slices. Bio-protocol. 2016; 6:e1730. [PubMed: 27158639]

41. Engelhart WG. Microwave hydrolysis of peptides and proteins for amino acid analysis. Am Biotechnol Lab. 1990; 8(15):30, 32, 34.

42. Yang, Y. Department of Toxicology and Cancer Biology. Univerisity of Kentucky; 2017. Metabolic Reprogramming of Human Lung Cancer Cells and ex vivo Tissues Revealed by UHR-FTMS Analysis of Small Amino and Carboxyl Metabolites.

43. Moseley HN. Correcting for the effects of natural abundance in stable isotope resolved metabolomics experiments involving ultra-high resolution mass spectrometry. BMC Bioinformatics. 2010; 11:139. [PubMed: 20236542]

44. Takeshita H, Horiuchi M, Izumo K, Kawaguchi H, Arimura E, Aoyama K, Takeuchi T. Long-term voluntary exercise, representing habitual exercise, lowers visceral fat and alters plasma amino acid levels in mice. Environ Health Prev Med. 2012; 17(4):275–84. [PubMed: 22052204]

45. Labuschagne CF, van den Broek NJ, Mackay GM, Vousden KH, Maddocks OD. Serine, but not glycine, supports one-carbon metabolism and proliferation of cancer cells. Cell Rep. 2014; 7(4): 1248–58. [PubMed: 24813884]

46. Lawrence SA, Hackett JC, Moran RG. Tetrahydrofolate recognition by the mitochondrial folate transporter. J Biol Chem. 2011; 286(36):31480–9. [PubMed: 21768094]

Highlights

- Chloroformate-based UHR-FTMS method shows excellent linear response to amino acids.
- UHR-FTMS resolves simultaneous ^{13}C and ^{2}H isotopologues of amino acids in mSIRM.
- Method was used to characterize metabolic change in lung cancer cells and tissues.
- Characterized metabolic changes in cancer are consistent with previous reports.

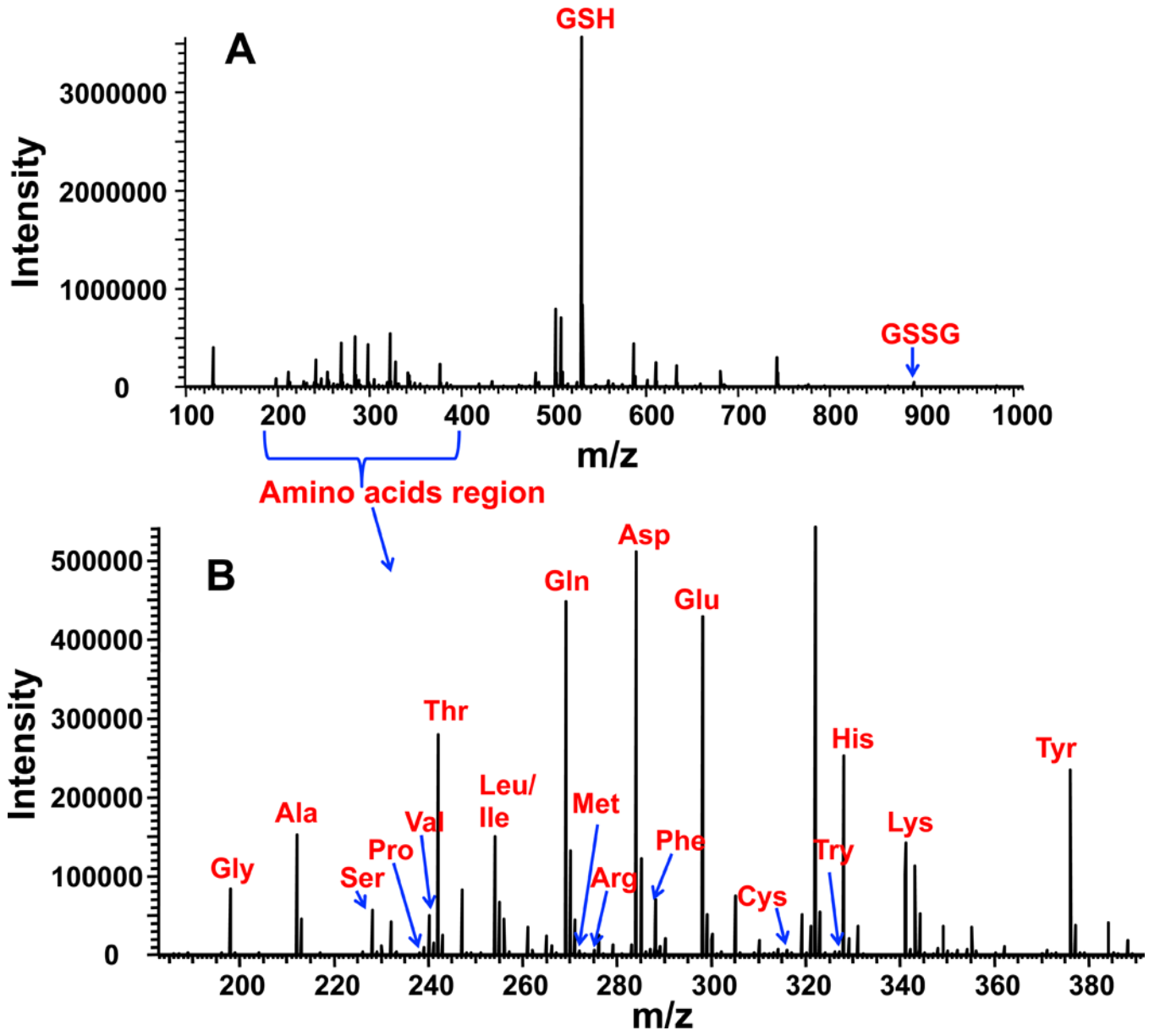

Figure 1. Typical positive ion mode spectrum of an unlabeled polar extract of PC9 cells after derivatization with ECF

Panel **A** shows the full m/z range profile spectrum, which included the Na adducts of GSH and GSSG derivatives along with amino acid derivatives. Panel **B** shows the zoom-in profile spectrum in the amino acid range. The m/z peaks were assigned using “PREMISE” [13]. Most of the amino acids shown represented Na adduct species except for Arg and His, which were protonated species.

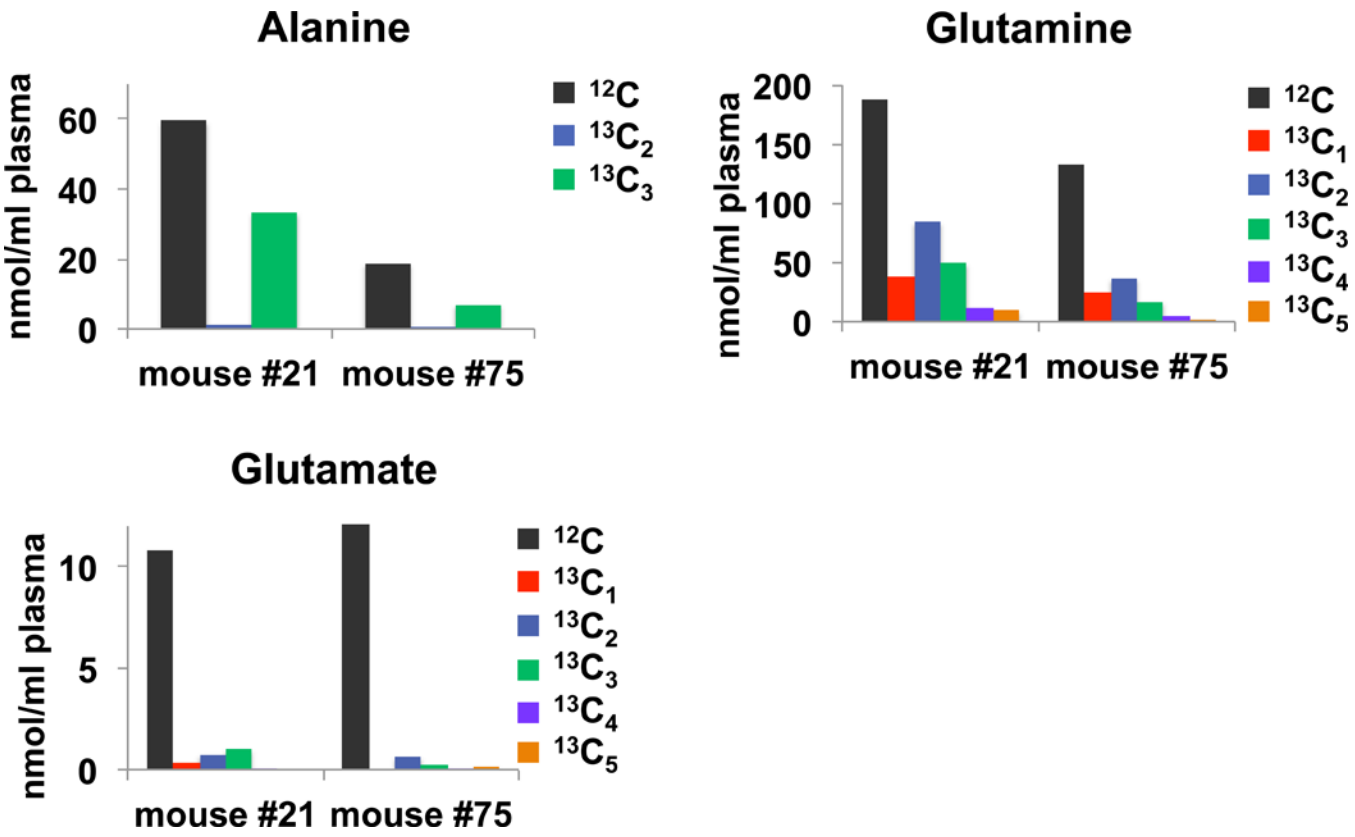

Figure 2. ^{13}C labeled amino acids in blood plasma of mice fed with a $^{13}C_6$-glucose diet

Blood plasma from mice fed with the $^{13}C_6$-glucose diet was obtained and treated as described in the methods. Isotopologues of the amino acids were determined via the ECF derivatives by UHR-FTMS. High ^{13}C enrichment was observed in Ala (ca. 33%) and Gln (ca. 50%) but not in Glu (<10–15%).

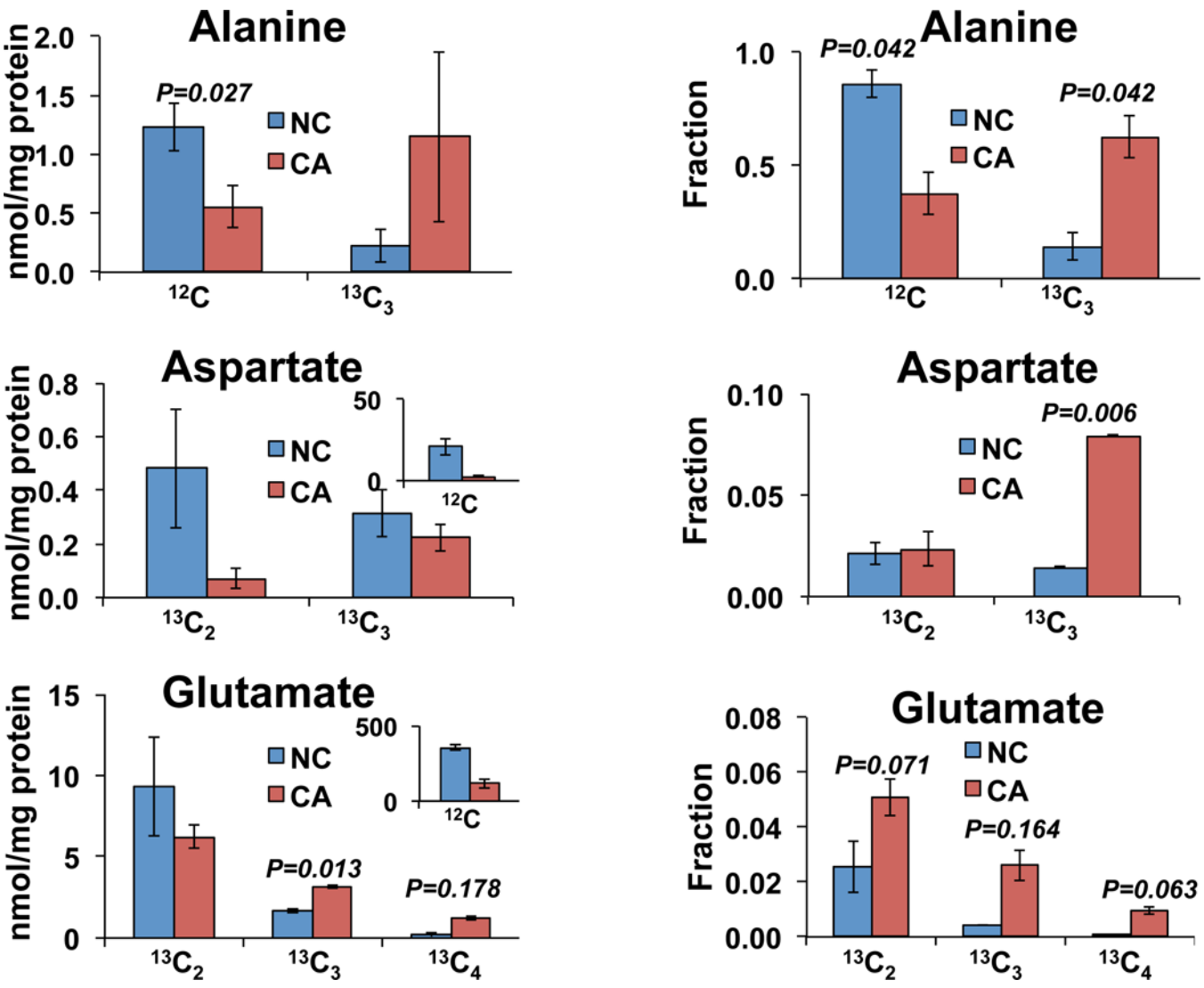

Figure 3. ^{13}C labeling in human lung tissues

The polar extract of lung tissues slices incubated for 24 h in the presence of $^{13}C_6$-glucose were processed as described in the methods. The amounts of different isotopologues of three amino acids were normalized to the tissue protein weight (left) and the fractional enrichments were calculated (right). Non-cancerous (NC, blue) and cancerous (CA, red) tissue slices procured from a lung cancer patient (UK018). N=2; error bars represent standard error of mean (SEM).

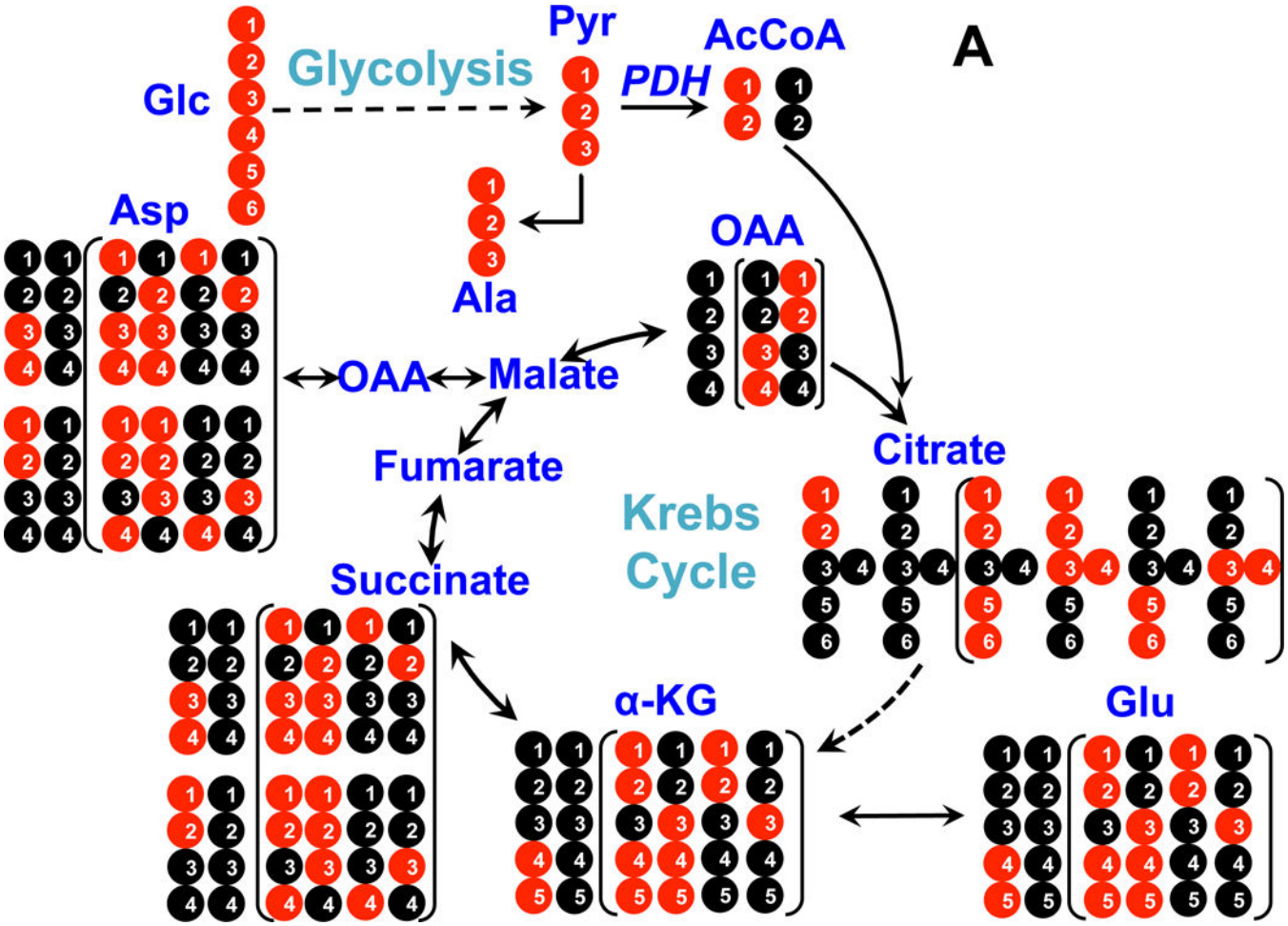

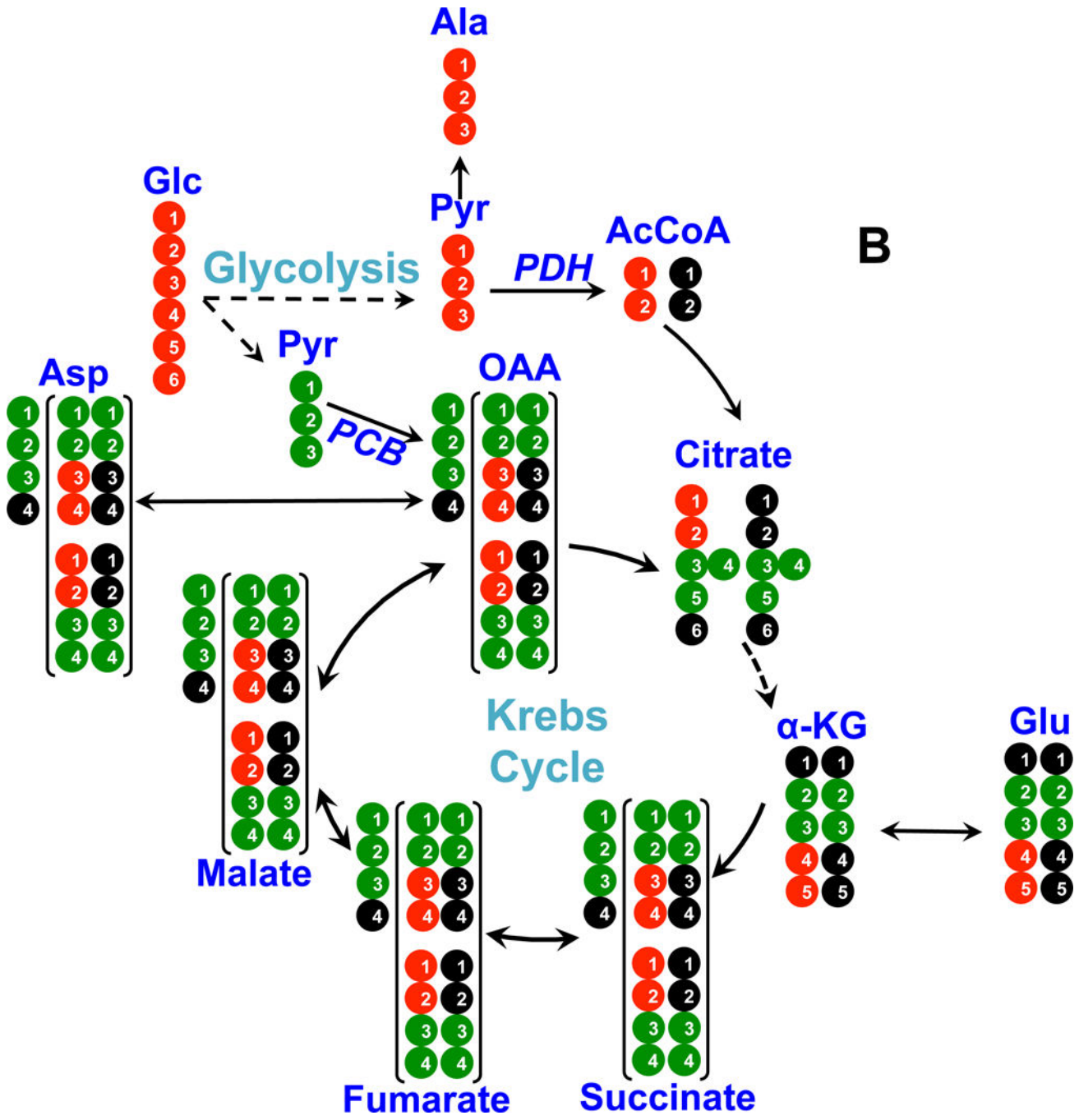

Figure 4. ^{13}C atom-resolved tracing of $^{13}C_6$-Glc oxidation through the interconnecting cytoplasmic glycolysis and mitochondrial Krebs cycle

Panel **A** shows ^{13}C incorporation from $^{13}C_6$-Glc into various metabolites via the PDH (pyruvate dehydrogenase) pathway; panel **B** shows ^{13}C incorporation from $^{13}C_6$-Glc into metabolites via the PCB (pyruvate carboxylase) pathway. ●: ^{12}C; ●: ^{13}C; ●,● indicates ^{13}C derived from PDH or PCB mediated Krebs cycle reactions, respectively; In panel A, the labeled patterns of the first and second (in brackets) turns of the PDH-initiated Krebs cycle are shown. In panel B, $^{13}C_3$-pyruvate (Pyr) is carboxylated to form $^{13}C_3$-

oxaloacetate (OAA), leading to the formation of $^{13}C_3$-Asp, -malate, -fumarate, and -succinate (patterns outside brackets); the labeled structures in brackets are derived from the reaction of $^{13}C_3$-OAA with $^{13}C_2$- or unlabeled acetyl CoA (AcCoA) to form other labeled Krebs cycle intermediates after one cycle turn. α-KG: α-ketoglutarate; not all expected labeled patterns of metabolites are shown [10].

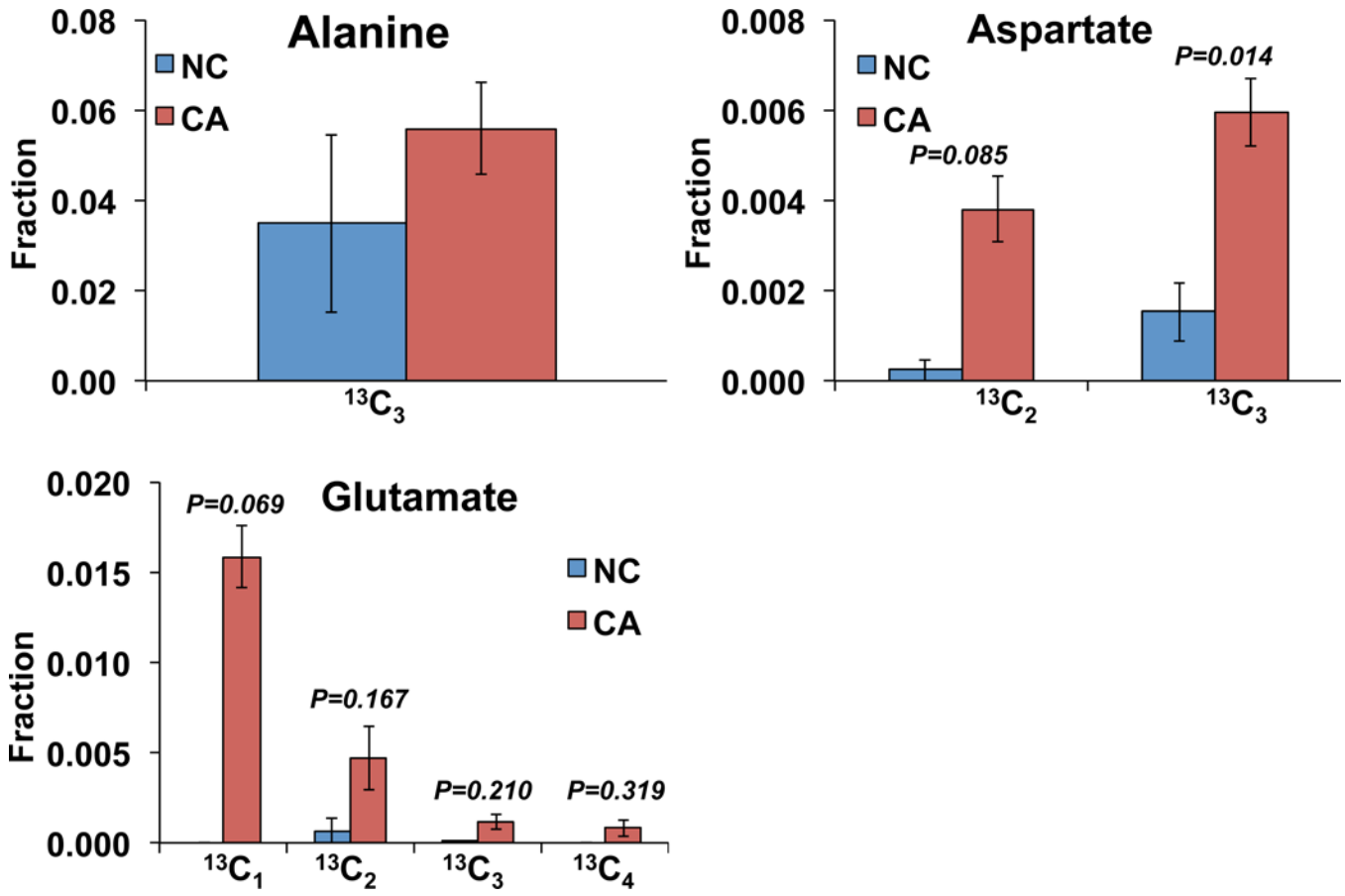

Figure 5. Fractional enrichment of isotopologues in different amino acids hydrolyzed from non-cancerous or cancerous tissue proteins

N=2; error bars represent SEM.

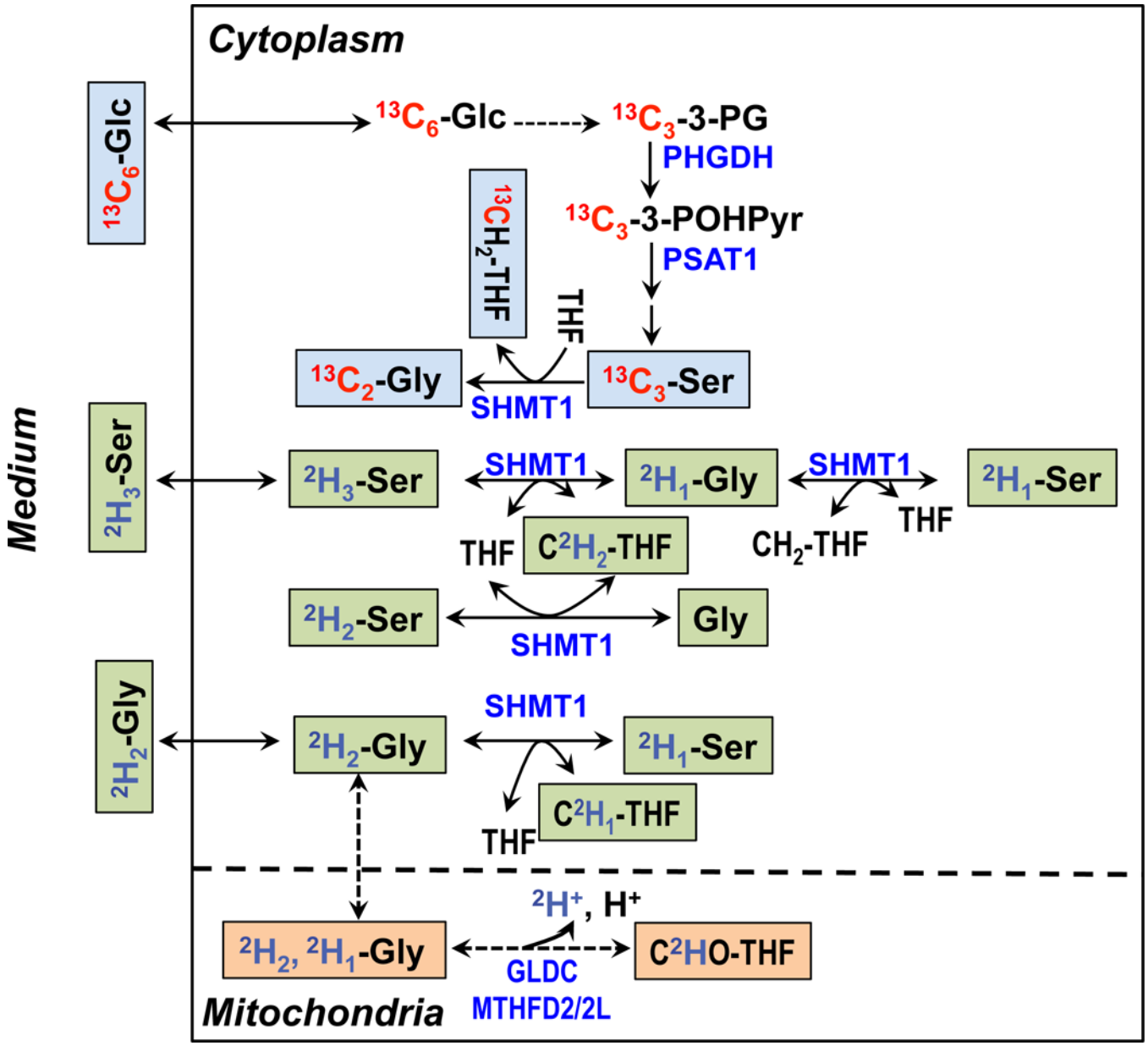

Figure 6. De novo synthesis of Ser and Gly from glucose via glycolysis and the 3-phosphoglycerate (3-PG) pathway and exchanges of exogenously derived Ser and Gly via one-carbon metabolism

Selected Ser and Gly exchange reactions are depicted for the cytoplasmic and mitochondrial compartments to illustrate the production of different 2H isotopologues of Gly and Ser in Figs. 7 and 8. For example, the serine hydroxymethyl transferase (SHMT) reaction was shown for the cytoplasm (SHMT1) but omitted for the mitochondria (SHMT2) [10, 46]. Blue text blocks depict the de novo synthesis carbon pathway from $^{13}C_6$-glucose while green and beige text blocks respectively depict the hydrogen exchange pathway of Gly and Ser via 1-carbon metabolism catalyzed by SHMT1, glycine decarboxylase complex (GLDC), and methylenetetrahydrofolate dehydrogenase (MTHFD). PHGDH: phosphoglycerate dehydrogenase; PSAT1: phosphoserine amino transferase 1; MTHFD2:

mitochondrial NAD^+-dependent methylene tetrahydrofolate dehydrogenase/methylene tetrahydrofolate cyclohydrolase; MTHFD2L: mitochondrial $NADP^+$-dependent methylene tetrahydrofolate dehydrogenase.

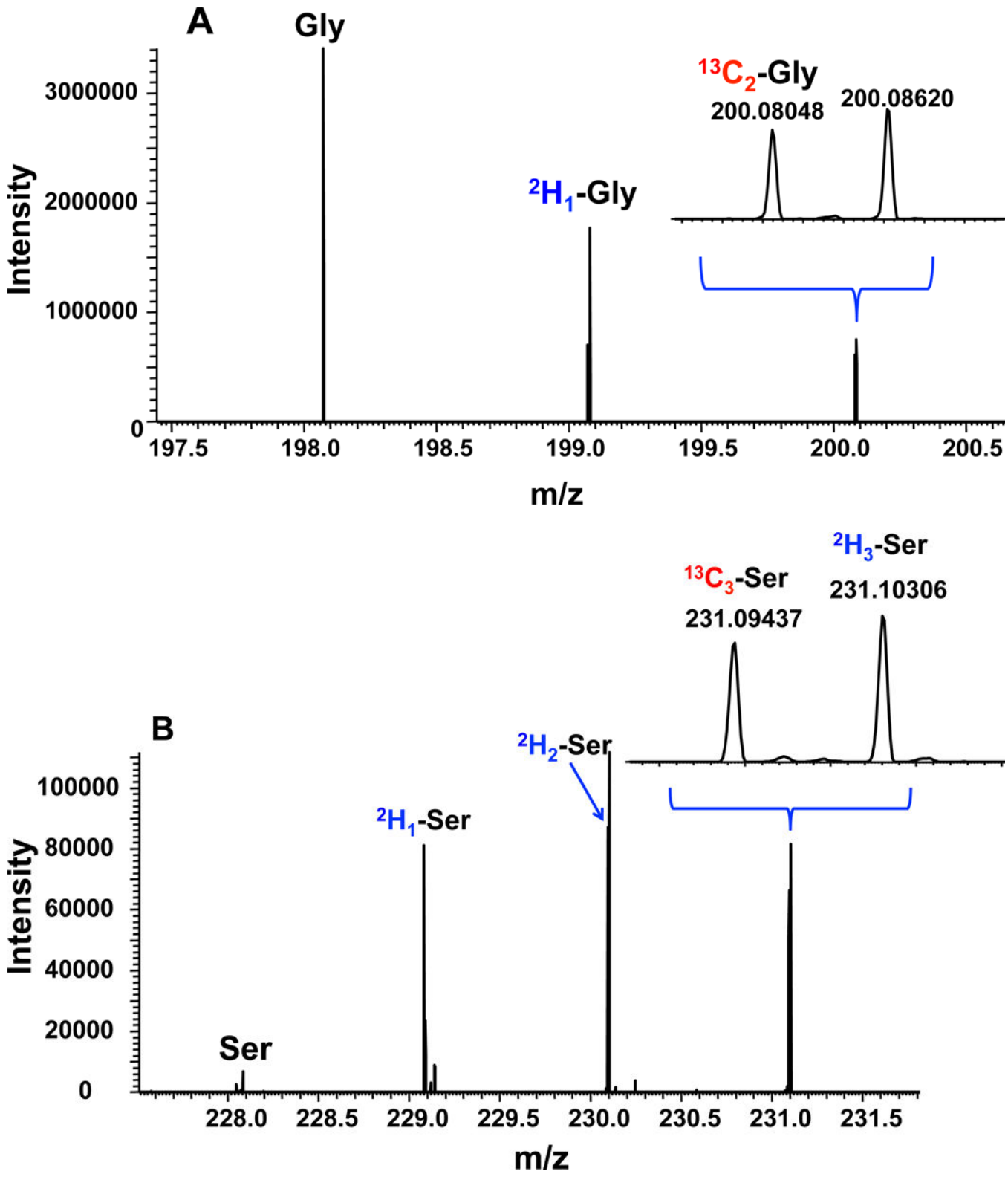

Figure 7. UHR-FTMS of an extract of PC9 cells

Panel **A** shows the UHR-FTMS profile spectrum of the Gly-ECF region of a polar extract of PC9 cells grown in a medium containing $^{13}C_6$-Glc+$^{2}H_2$-Gly. Panel **B** shows the UHR-FTMS profile spectrum of the Ser-ECF region of a polar extract of $^{13}C_6$-Glc+$^{2}H_3$-Ser labeled PC9 cells.

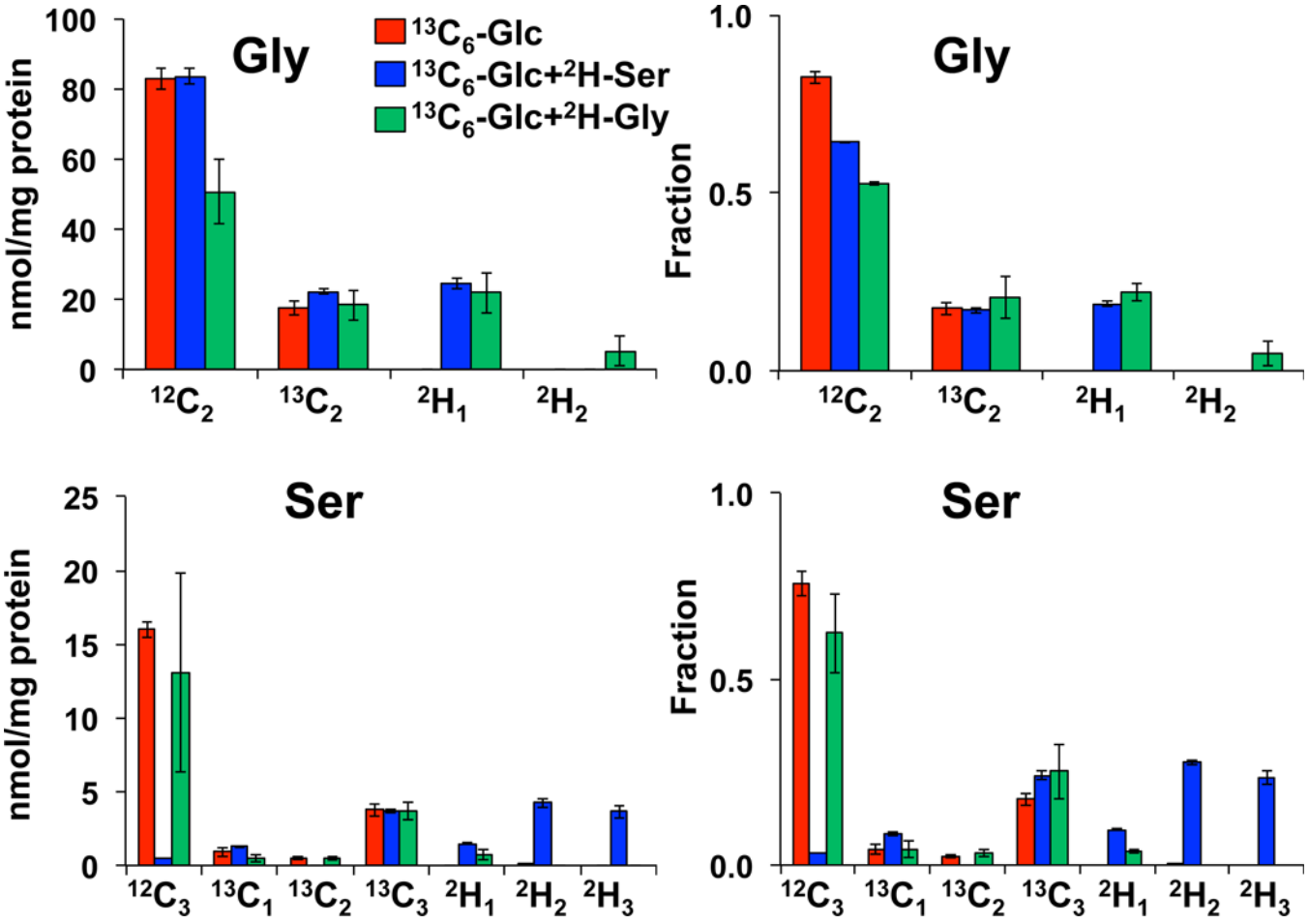

Figure 8.

^{13}C and ^2H Isotopologue distribution of Ser and Gly in dually labeled PC9 cell extracts indicates extensive exchanges between the two amino acids. N=3; error bars represent SEM.

Table 1

Linearity of response of the ECF-derivatized amino acids standard

Amino acids	N	Linear range (nM)	R^2
Ala	4	5-5000	0.995
Arg	4	5-5000	0.999
Asn	4	5-5000	0.997
Asp	4	5-5000	0.998
Cystine	4	5-1250	0.988
Glu	4	5-5000	0.990
Gln	4	5-5000	0.997
Gly	4	5-5000	0.994
His	4	5-5000	0.999
Leu+Ile	4	5-5000	0.999
Lys	4	5-5000	0.999
Met	4	5-5000	0.999
Phe	4	5-5000	1.000
Pro	4	5-5000	0.999
Ser	4	5-5000	0.992
Thr	4	5-5000	0.987
Trp	4	5-5000	0.998
Tyr	4	5-5000	1.000
Val	4	5-5000	0.997